ELSEVIER

Shape sensitivities in the reliability analysis of nonlinear frame structures

Terje Haukaas [a,*], Michael H. Scott [b]

[a] Department of Civil Engineering, University of British Columbia, 6250 Applied Science Lane, Vancouver, BC, Canada V6T 1Z4
[b] Department of Civil, Construction, and Environmental Engineering, Oregon State University, Corvallis, OR 97331, United States

Abstract

A unified and comprehensive treatment of shape sensitivity that includes variations in the nodal coordinates, member cross-section properties, and global shape parameters of inelastic frame structures is presented. A novelty is the consideration of geometric uncertainty in both the displacement- and force-based finite element formulations of nonlinear beam-column behavior. The shape sensitivity equations enable a comprehensive investigation of the relative influence of uncertain geometrical imperfections on structural reliability assessments. For this purpose, finite element reliability analyses are employed with sophisticated structural models, from which importance measures are available. The unified approach presented herein is based on the direct differentiation method and includes variations in the equilibrium and compatibility relationships of frame finite elements, as well as the member cross-section geometry, in order to obtain complete shape sensitivity equations. The analytical shape sensitivity equations are implemented in the OpenSees software framework. Numerical examples involving a steel structure and a reinforced concrete structure confirm that geometrical imperfections may have a significant impact on structural reliability assessments.
© 2006 Elsevier Ltd. All rights reserved.

Keywords: Shape sensitivity; Direct differentiation method; Geometrical imperfections; Structural reliability; Beam-columns; Nonlinear analysis; OpenSees

1. Introduction

A number of applications in structural engineering require the computation of the gradient of structural response quantities with respect to input parameters. This is referred to as response sensitivity analysis. The most common applications of response sensitivity analysis are to optimization problems, such as the minimization of structural cost subject to constraints and minimization of the difference between measured and numerical response for system identification purposes. Yet another optimization problem is posed in structural reliability analysis by the first and second-order reliability methods (FORM and SORM). These methods rely upon the determination of the "most probable failure point", which is the solution to a constrained optimization problem in the space of random variables. As a by-product, FORM analysis provides importance measures to rank the uncertain parameters according to their relative influence on the structural reliability. Importance measures remedy the problem that individual response sensitivities cannot be compared directly due to differing units. It is also emphasized that response sensitivities are useful as a stand alone product in structural design because they indicate the sensitivity of a structural response quantity to changes in the design parameters.

Three requirements are put forward by the application of response sensitivities in gradient-based optimization algorithms: efficiency, accuracy, and consistency. Efficient

---

* Corresponding author. Tel.: +1 604 827 5557; fax: +1 604 822 6901.
  E-mail addresses: terje@civil.ubc.ca (T. Haukaas), michael.scott@oregonstate.edu (M.H. Scott).

computation of response sensitivities is required to make gradient-based algorithms competitive with gradient-free methods, including response surface methods, in terms of computational cost. This is particularly important when the optimization is performed in a high-dimensional space of variables, in which case repeated runs to obtain gradients by finite differences is infeasible. Accuracy is imperative to avoid convergence problems in the optimization algorithms, which tend to perform poorly in the presence of even small inaccuracies in the gradients. The consistency requirement stems from the utilization of approximate numerical models to obtain the structural response. Because it is the approximate response that is employed in the optimization problem, it is the gradient of the approximate response that is required. Consequently, it is not of interest to pursue the "exact" gradient of the theoretical boundary value problem. In fact, this would lead to inconsistency between the function value and its gradient.

Two approaches are available to obtain response sensitivities: finite difference methods (FDMs) and the direct differentiation method (DDM). The finite difference approach employs re-runs of the structural analysis with perturbed parameter values to estimate the response sensitivity. As a result, it is a computationally inefficient approach. Moreover, FDMs suffer from accuracy concerns. It is a nontrivial task to select the value of the parameter perturbation for nonlinear problems. If the perturbation is too small, round-off errors are introduced; while if the perturbation is too large, local nonlinearities may lead to inaccurate estimates of the sensitivity. The consistency requirement, however, is satisfied by the FDMs because it is the approximate response that is employed in the finite difference equations.

The DDM provides an attractive alternative to FDMs. At the one-time cost of deriving and implementing analytical sensitivity equations within the finite element response algorithm, efficient, accurate, and consistent response sensitivities are obtained. No finite difference computations take place within the DDM; instead, the response equations are analytically differentiated and implemented on the computer alongside the ordinary response computations. A number of researchers have contributed to the development of such analytical equations, including Choi and Santos [2], Tsay and Arora [24], Liu and Der Kiureghian [15], Zhang and Der Kiureghian [25], Kleiber et al. [13], Conte et al. [3], Roth and Grigoriu [20], Scott et al. [22], and Haukaas and Der Kiureghian [9]. The DDM is more efficient than FDMs because repeated runs of the response analysis are unnecessary. Accuracy is ensured at the same precision as the response because the same equation solver is employed to obtain both the response and the response sensitivity. Consistency is achieved by differentiating the response equations after they have been spatially and temporally discretized by the finite element procedures. The DDM is thus the preferred approach to computing response sensitivities.

In this paper, the OpenSees software framework [16] is extended and applied for shape sensitivity analysis. OpenSees (open system for earthquake engineering simulation) is an open-source, object-oriented, general-purpose finite element code specifically developed for earthquake engineering analysis. OpenSees began as the computational platform for testbed simulations in the Pacific Earthquake Engineering Research Center (PEER) and has since been adopted by the NSF-sponsored George E. Brown Jr. Network for Earthquake Engineering Simulation (NEES). Work by Haukaas and Der Kiureghian [8] extends OpenSees with response sensitivity and reliability analysis capabilities which allow the analyst to characterize input parameters as random variables and compute probabilities of structural response events. This is termed finite element reliability analysis (FERA), which differs from so-called stochastic finite element methods that focus on second-moment statistics of the response. In contrast, reliability analysis and specifically FERA is suited to compute probabilities of rare response events. This addresses the growing demand in performance-based engineering to assess structural behavior during rare events of intense loading in a probabilistic manner.

The response sensitivity implementations in OpenSees are based on the DDM. The implementations are divided into an overarching framework and object-specific implementations. The latter reflect the fact that OpenSees is organized into element, section, and material objects. The framework for sensitivity computations, as well as specific implementations for selected elements, sections, and materials, is already in place. This includes sensitivities with respect to nodal coordinates, which previous studies suggest may be an important source of uncertainty in structural reliability, particularly when nonlinear structural behavior is considered [9].

In this paper, the DDM shape sensitivity equations include response sensitivities with respect to: (1) nodal coordinates, (2) global structural or member shape parameters, and (3) the dimensions and details of fiber-discretized cross-sections. Of particular significance is the development of unified shape sensitivity equations for beam-column elements in both the displacement- and force-based formulations. Gradient computations that incorporate shape sensitivity at all levels (structure, element, and section) are presented and their implementation in OpenSees allows the inclusion of a wide range of uncertain geometrical imperfections in a reliability analysis. Two numerical examples involving a steel structure and a reinforced concrete structure provide insight into the importance of uncertain geometrical imperfections relative to other uncertain structural properties.

2. The application of response sensitivities in finite element reliability analysis

The need for response sensitivities in this paper stems from structural reliability analysis. To achieve accurate

reliability assessments, sophisticated structural models are employed to simulate structural performance. Clearly, such predictions can only be made in a probabilistic sense due to uncertainties in the model and the input parameters. This motivates the utilization of FERA to obtain probabilistic predictions of response events. Indeed, the emerging performance-based engineering approach is envisioned to be implemented in a reliability framework [6,17]. The primary objective in FERA is to obtain the probability of rare response events that are identified by user-defined performance functions. An important by-product of the analysis is parameter importance measures to rank the variables according to their relative importance. Response sensitivities represent an essential ingredient in the analysis, as described in the following.

The reliability problem for the case of a single-performance function is formulated as the multi-fold integral

$$p = \int \cdots \int_{g \leqslant 0} f(\mathbf{\Theta}) \, \mathrm{d}\mathbf{\Theta}, \tag{1}$$

where p is the sought probability, g is the performance function that identifies the response event for which the probability is sought, and $f(\mathbf{\Theta})$ is the joint probability density function for the random variables, which are collected in the vector $\mathbf{\Theta}$. In FERA the performance function is specified in terms of response quantities $\mathbf{U} = \mathbf{U}(\mathbf{\Theta})$ from a finite element analysis. The random variables are commonly specified by marginal probability distributions and correlation coefficients. Analytical solutions to Eq. (1) are unavailable; however, methods such as FORM and SORM and sampling techniques provide approximate solutions. Of particular interest in finite element reliability analysis is FORM, followed by efficient importance sampling to correct for potential nonlinearities. This analysis strategy is beneficial because it requires relatively few evaluations of the performance function and, in effect, few executions of the finite element analysis. Moreover, FORM analysis generates the parameter importance measures that are utilized in this paper.

In FORM, the integration boundary $g = 0$ in Eq. (1) is approximated by a hyperplane in the transformed space $\mathbf{Y} = \mathbf{Y}(\mathbf{\Theta})$ of uncorrelated standard normal random variables. For nonlinear performance functions, the ideal point of approximation is the point on the surface $g = 0$ that is closest to the origin in the $\mathbf{Y}$-space. This point, termed the most likely failure point (MPP) and denoted $\mathbf{Y}^*$, is the solution to the constrained optimization problem

$$\mathbf{Y}^* = \mathrm{argmin}\{\|\mathbf{Y}\| \mid g = 0\}. \tag{2}$$

The most efficient algorithms available to solve this optimization problem utilize the gradient of the performance function; namely, $\nabla g = \partial g / \partial \mathbf{Y}$. The chain rule of differentiation applied to the performance function yields

$$\frac{\partial g}{\partial \mathbf{Y}} = \frac{\partial g}{\partial \mathbf{U}} \frac{\partial \mathbf{U}}{\partial \mathbf{\Theta}} \frac{\partial \mathbf{\Theta}}{\partial \mathbf{Y}}. \tag{3}$$

The derivative $\partial g / \partial \mathbf{U}$ is readily available since g is a simple algebraic function of the response quantities $\mathbf{U}$. The matrix $\partial \mathbf{U} / \partial \mathbf{\Theta}$ signifies the need to compute response gradients, which is the focus this paper, and the matrix $\partial \mathbf{\Theta} / \partial \mathbf{Y}$ is the Jacobian of the probability transformation. The Nataf transformation [14] is applied in this work, for which the required Jacobian matrix is already available in OpenSees. This transformation is an attractive alternative to the Rosenblatt transformation [19,10] because it allows a wider range of correlation values for a variety of probability distribution types. The communication between the reliability algorithm and the finite element module consists of updating the finite element model with realizations of the random variables $\mathbf{\Theta}$ and returning $\mathbf{U}$ and $\partial \mathbf{U} / \partial \mathbf{\Theta}$ each time the performance function is evaluated.

Upon determination of $\mathbf{Y}^*$, the probability p according to FORM is determined by

$$p = \Phi(-\beta), \tag{4}$$

where Φ is the standard normal cumulative distribution function and β is the reliability index defined in FORM as $\beta = \|\mathbf{Y}^*\|$. Importance sampling with the sampling distribution centered at $\mathbf{Y}^*$ may subsequently be performed since it is an efficient scheme compared with Monte Carlo sampling centered at the mean realization of the random variables.

The developments in this paper allow the characterization of imperfections in nodal coordinates and member cross-section geometry as random variables, in addition to random material and load variables. Of particular interest is the investigation of the importance of these variables relative to other sources of uncertainty. Clearly, the components of the vectors $\partial U / \partial \mathbf{\Theta}$ cannot be employed for this purpose due to the differing dimensions of the variables $\theta \in \mathbf{\Theta}$. Instead, importance measures from FORM are utilized, in which the components have uniform dimensions. The basis for these measures are presented by Hohenbichler and Rackwitz [11] and Bjerager and Krenk [1]. Applications of importance measures in FERA is presented by Haukaas and Der Kiureghian [9], where the following vector ranks the random variables:

$$\gamma = -\frac{\partial g}{\partial \mathbf{Y}} \boldsymbol{J}_{\mathbf{Y}^*, \theta^*} \sqrt{\mathrm{diag}\left(\boldsymbol{J}_{\mathbf{Y}^*, \theta^*}^{-1} \boldsymbol{J}_{\mathbf{Y}^*, \theta^*}^{-\mathrm{T}}\right)}, \tag{5}$$

where $\partial g / \partial \mathbf{Y}$ is provided by Eq. (3), $\boldsymbol{J}_{\mathbf{Y}^*, \theta^*}$ is the Jacobian matrix of the probability transformation at the MPP, and $\sqrt{}$ implies the square root of each element of the argument matrix. It is noted that γ reduces to $-\partial g / \partial \mathbf{Y}$, which is a scaled version of the well known "alpha-vector" in reliability analysis when no correlation between the random variables is present. Furthermore, it is common to scale the γ-vector so that $\|\gamma\| = 1$. The elements of γ are interpreted as the contributions from the individual random variables on the reliability of the structure. Moreover, a negative (positive) γ-component indicates that the corresponding random variable acts as a resistance (load) variable.

3. Top-level response sensitivity equations

The gradient of the performance function in Eq. (3) signifies the need to compute sensitivities of the structural response, $\partial \mathbf{U}/\partial \mathbf{\Theta}$. To compute the response sensitivity by the DDM, the equations that govern the structural response are differentiated. For the set of parameters $\mathbf{\Theta}$ that describe the material, geometric, and load parameters of a structural model, the global equations of static equilibrium have the form

$$\mathbf{P}_r(\mathbf{U}(\mathbf{\Theta}), \mathbf{\Theta}) = \mathbf{P}_f(\mathbf{\Theta}), \tag{6}$$

where $\mathbf{P}_r$ is the vector of internal resisting forces of the structure. The internal forces may depend explicitly upon $\mathbf{\Theta}$, as well as implicitly through the nodal displacement response vector $\mathbf{U}$. The vector $\mathbf{P}_f$ represents the external loads applied to the structure. Inertial and damping forces are omitted from Eq. (6) because dynamic equilibrium effects are independent of the element and section formulations considered in this paper. The extension of Eq. (6) to dynamic equilibrium and the computation of the corresponding response sensitivity are straightforward [5].

To formulate the equations for response sensitivities at the structural level, Eq. (6) is differentiated with respect to any parameter θ selected from the vector $\mathbf{\Theta}$:

$$\frac{\partial \mathbf{P}_r}{\partial \mathbf{U}} \frac{\partial \mathbf{U}}{\partial \theta} + \frac{\partial \mathbf{P}_r}{\partial \theta}\bigg|_{\mathbf{U}} = \frac{\partial \mathbf{P}_f}{\partial \theta}. \tag{7}$$

The explicit and implicit dependence of $\mathbf{P}_r$ on θ are taken into account by the chain rule of differentiation. The vector $\partial \mathbf{P}_r/\partial\theta|_{\mathbf{U}}$ is the derivative of the resisting forces conditioned upon fixed displacements. This vector is assembled from element contributions in the same manner as the resisting force vector itself. The vector $\partial \mathbf{P}_f/\partial\theta$ is the derivative of the external load, which is nonzero only when the parameter θ represents a load applied to the structure. Rearrangement of Eq. (7) gives a linear system of equations for the nodal response sensitivity $\partial \mathbf{U}/\partial\theta$ [13]:

$$\mathbf{K}_T \frac{\partial \mathbf{U}}{\partial \theta} = \frac{\partial \mathbf{P}_f}{\partial \theta} - \frac{\partial \mathbf{P}_r}{\partial \theta}\bigg|_{\mathbf{U}}, \tag{8}$$

where $\mathbf{K}_T = \partial \mathbf{P}_r/\partial \mathbf{U}$ is the tangent stiffness matrix. For each parameter in the vector $\mathbf{\Theta}$, assembly of the right-hand side and solution of the factorized system of equations in Eq. (8) gives the corresponding nodal response sensitivity vector. The linear form of Eq. (8) and the reuse of the factorized tangent stiffness matrix contribute to the computational efficiency of the DDM.

The sensitivity equation in Eq. (8) requires the assembly of derivatives of the force vector $\mathbf{p}$ from each element, for fixed nodal displacements:

$$\frac{\partial \mathbf{P}_r}{\partial \theta}\bigg|_{\mathbf{U}} = \bigcup_{\text{num. el.}} \frac{\partial \mathbf{p}}{\partial \theta}\bigg|_{\mathbf{u}}, \tag{9}$$

where $\cup$ denotes the assembly procedure and $\mathbf{u}$ is the element displacement vector. It is noted that assembly is required over all elements that contain inelastic material response, regardless of whether θ corresponds to a parameter for the individual elements. The one-to-one mapping that exists between the vectors $\mathbf{U}$ and $\mathbf{u}$ is independent of θ and therefore does not require differentiation. The key to computing response sensitivities by the DDM is to obtain $\partial \mathbf{p}/\partial\theta|_{\mathbf{u}}$ from each element in the structural model. The computation of $\partial \mathbf{p}/\partial\theta|_{\mathbf{u}}$ depends upon the element formulation for inelastic material response, as described in the following sections.

4. Overview of element equilibrium and kinematic equations

An overview of the equilibrium and compatibility equations required to assemble the resisting force vector from element contributions is shown in Fig. 1, where the presentation follows that of Filippou and Fenves [4]. The equations on the left-hand side of Fig. 1 represent equilibrium between the internal forces at the different levels while those on the right-hand side of the figure represent the compatibility relationships between the deformations at each level. The middle column of Fig. 1 shows the constitutive relationships that link the forces and deformations at each level.

In the global system, the resisting forces and nodal displacements of an element are contained in the vectors $\mathbf{p}$ and $\mathbf{u}$, respectively. It is common to formulate beam-column elements in a basic system, free of rigid body displacement modes, where the element deformations are collected in the vector $\mathbf{v}$ and the corresponding forces in the vector $\mathbf{q}$. For small displacements, the compatibility relationship between nodal displacements and element deformations is linear, as described by the matrix–vector product $\mathbf{v} = \mathbf{A}\mathbf{u}$. The matrix $\mathbf{A}$ describes the transformation of forces and displacements between the global and basic systems as defined by the element orientation in the global coordinate system. The contra-gradient relationship $\mathbf{p} = \mathbf{A}^T\mathbf{q}$ gives equilibrium between element forces in the basic and global systems.

The matrices $\mathbf{a}_e$ and $\mathbf{b}$ shown in Fig. 1 describe the equilibrium and compatibility relationships within the basic system of the element, as discussed later in this paper. The section compatibility matrix, $\mathbf{a}_s$, relates section deformations to material strain at any point on the cross-sectional area.

5. Unified approach for sensitivity derivations

As indicated in Eq. (9), response sensitivity analysis by the DDM requires the conditional derivative of $\mathbf{p}$ for fixed $\mathbf{u}$ be computed for each element in the structural model. When the parameter θ represents a material property, and standard finite element formulations are employed, it is sufficient to differentiate directly the equilibrium equations and the material constitutive law under the condition of fixed displacements and strains [13] in order to determine $\partial \mathbf{p}/\partial\theta|_{\mathbf{u}}$. Furthermore, as recognized by Haukaas and Der Kiureghian [7], in order to obtain correct sensitivity results
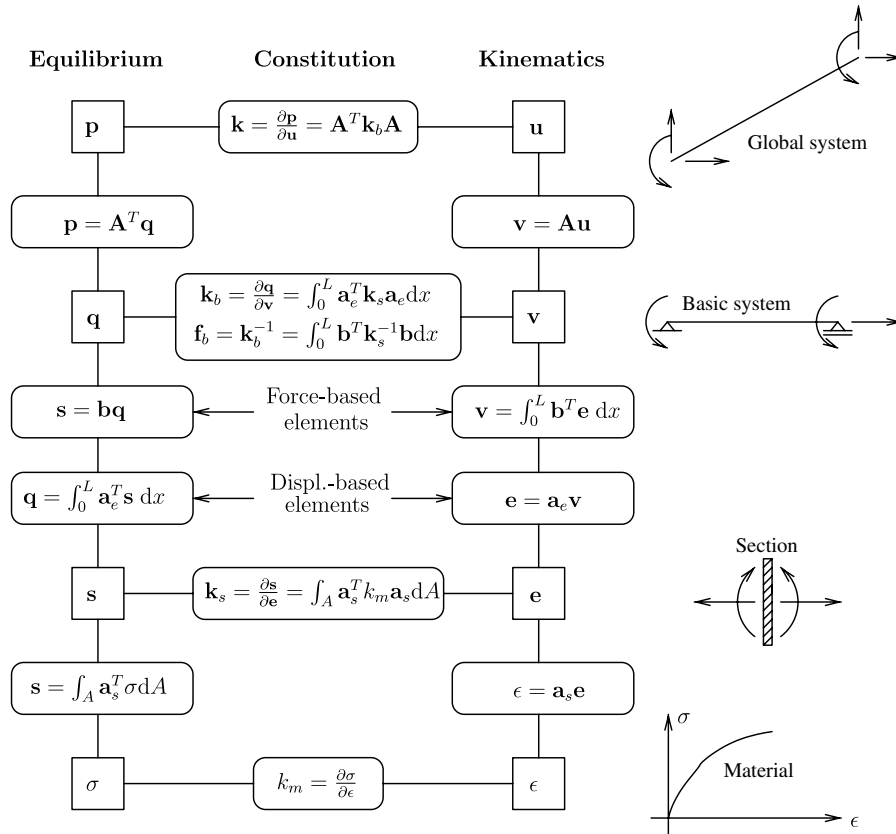
Fig. 1. Governing equations for beam-column elements.

in cases where θ represents a geometric parameter, the kinematic relationships must also be differentiated under the condition of fixed displacements.

Although the above approach provides correct results for displacement-based finite elements, it is not applicable in the force-based formulation, where the displacement field is unspecified. The approach taken herein to deriving the shape sensitivity equations is to combine the complete derivatives of the element force vectors with the derivatives of the equilibrium and compatibility relationships that link each level in Fig. 1. Originally developed by Scott et al. [22] for the case where θ represents a material parameter, the derivation is extended in this paper to include cases where θ represents a geometric parameter. This approach essentially consists of combining four equations at each level of Fig. 1. In summary, these equations are

(a) The derivative of the equilibrium equation.
(b) The derivative of the kinematic compatibility equation.
(c) The complete derivative of the force vector at the present level to include the constitutive law.
(d) The complete derivative of the force vector at the level below to link to the lower level.

This approach is demonstrated for the conditional derivative of the global element forces, $\partial\mathbf{p}/\partial\theta|_\mathbf{u}$. The deriv-

atives of the equilibrium and compatibility relationships between the global configuration and the basic system are

$$\frac{\partial\mathbf{p}}{\partial\theta} = \mathbf{A}^{\mathrm{T}}\frac{\partial\mathbf{q}}{\partial\theta} + \frac{\partial\mathbf{A}^{\mathrm{T}}}{\partial\theta}\mathbf{q}, \tag{10a}$$

$$\frac{\partial\mathbf{v}}{\partial\theta} = \mathbf{A}\frac{\partial\mathbf{u}}{\partial\theta} + \frac{\partial\mathbf{A}}{\partial\theta}\mathbf{u}, \tag{10b}$$

while the complete derivatives of the global and basic forces are

$$\frac{\partial\mathbf{p}}{\partial\theta} = \frac{\partial\mathbf{p}}{\partial\mathbf{u}}\frac{\partial\mathbf{u}}{\partial\theta} + \frac{\partial\mathbf{p}}{\partial\theta}\bigg|_\mathbf{u}, \tag{10c}$$

$$\frac{\partial\mathbf{q}}{\partial\theta} = \frac{\partial\mathbf{q}}{\partial\mathbf{v}}\frac{\partial\mathbf{v}}{\partial\theta} + \frac{\partial\mathbf{q}}{\partial\theta}\bigg|_\mathbf{v}. \tag{10d}$$

First, Eq. (10a) is expanded by inserting the derivatives of the global and basic forces, defined in Eqs. (10c) and (10d), respectively:

$$\mathbf{k}_\mathrm{g}\frac{\partial\mathbf{u}}{\partial\theta} + \frac{\partial\mathbf{p}}{\partial\theta}\bigg|_\mathbf{u} = \mathbf{A}^{\mathrm{T}}\mathbf{k}_\mathrm{b}\frac{\partial\mathbf{v}}{\partial\theta} + \mathbf{A}^{\mathrm{T}}\frac{\partial\mathbf{q}}{\partial\theta}\bigg|_\mathbf{v} + \frac{\partial\mathbf{A}^{\mathrm{T}}}{\partial\theta}\mathbf{q}, \tag{11}$$

where $\mathbf{k}_\mathrm{g} = \partial\mathbf{p}/\partial\mathbf{u}$ and $\mathbf{k}_\mathrm{b} = \partial\mathbf{q}/\partial\mathbf{v}$. This equation is then combined with Eq. (10b)

$$\mathbf{k}_\mathrm{g}\frac{\partial\mathbf{u}}{\partial\theta} + \frac{\partial\mathbf{p}}{\partial\theta}\bigg|_\mathbf{u} = \mathbf{A}^{\mathrm{T}}\mathbf{k}_\mathrm{b}\mathbf{A}\frac{\partial\mathbf{u}}{\partial\theta} + \mathbf{A}^{\mathrm{T}}\mathbf{k}_\mathrm{b}\frac{\partial\mathbf{A}}{\partial\theta}\mathbf{u} + \mathbf{A}^{\mathrm{T}}\frac{\partial\mathbf{q}}{\partial\theta}\bigg|_\mathbf{v} + \frac{\partial\mathbf{A}^{\mathrm{T}}}{\partial\theta}\mathbf{q}. \tag{12}$$

Then, the definition of the element stiffness matrix, $\mathbf{k}_g = \mathbf{A}^T \mathbf{k}_b \mathbf{A}$, simplifies this expression by cancellation of the terms involving $\partial \mathbf{u}/\partial \theta$, and the final expression for the conditional derivative of the element forces is

$$\left.\frac{\partial \mathbf{p}}{\partial \theta}\right|_{\mathbf{u}} = \mathbf{A}^T \mathbf{k}_b \frac{\partial \mathbf{A}}{\partial \theta} \mathbf{u} + \mathbf{A}^T \left.\frac{\partial \mathbf{q}}{\partial \theta}\right|_{\mathbf{v}} + \frac{\partial \mathbf{A}^T}{\partial \theta} \mathbf{q}. \tag{13}$$

The first and third terms on the right-hand side of Eq. (13) represent the sensitivity of the element forces to changes in the element length, as described by the matrix $\partial \mathbf{A}/\partial \theta$. This matrix is straightforward to compute from the direction cosines of the element and it is equal to zero for any parameter that does not represent a nodal coordinate for the element. The second term represents the link to the next level, the basic system, in which it is necessary to compute $\partial \mathbf{q}/\partial \theta|_{\mathbf{v}}$. This conditional derivative depends on the element formulation for nonlinear material behavior, as shown in the following sections for the displacement- and force-based beam-column formulations.

6. Gradient computations for displacement-based elements

The formulation of displacement-based beam-column elements follows standard finite element analysis procedures where the element displacement field is interpolated from the nodal displacements [12,26]. Compatible section deformations are interpolated from the element deformations, $\mathbf{e} = \mathbf{a}_e \mathbf{v}$, and there is weak equilibrium between the section and basic forces, $\mathbf{q} = \int_0^L \mathbf{a}_e^T \mathbf{s} \, dx$, as indicated in Fig. 1. For the standard interpolation fields of linear axial displacement and cubic Hermitian polynomial transverse displacement, the axial deformation is constant and the curvature is linear along the element, and the matrix $\mathbf{a}_e$ is

$$\mathbf{a}_e = \frac{1}{L} \begin{bmatrix} 1 & 0 & 0 \\ 0 & 6x/L - 4 & 6x/L - 2 \end{bmatrix}. \tag{14}$$

In the implementation of the displacement-based element the equilibrium relationship is evaluated by numerical integration (typically two-point Gauss integration) over the normalized domain $\xi = [-1, 1]$. The coordinate transformation between the x-domain and the ξ-domain reads $x = L/2(\xi + 1)$, where L is the element length. Hence, the Jacobian of the transformation is $dx/d\xi = L/2$, and the numerical integration of the equilibrium relationship is

$$\mathbf{q} = \sum_{i=1}^{N_p} \mathbf{a}_e^T(\xi_i) \mathbf{s}(\xi_i) \frac{L}{2} w_i, \tag{15}$$

where N_p is the number of integration points, ξ_i is the location of the ith integration point, and w_i is the associated integration weight. Both the points and weights are deterministic for Gauss integration, thus their derivatives will be equal to zero.

Further simplification of Eq. (15) is possible by substituting the x–ξ coordinate transformation into the matrix $\mathbf{a}_e$, in which case the equilibrium relationship becomes:

$$\mathbf{q} = \sum_{i=1}^{N_p} \tilde{\mathbf{a}}_e^T(\xi_i) \mathbf{s}(\xi_i) w_i, \tag{16}$$

where the normalized interpolation matrix is

$$\tilde{\mathbf{a}}_e = \frac{1}{2} \begin{bmatrix} 1 & 0 & 0 \\ 0 & 3\xi - 1 & 3\xi + 1 \end{bmatrix}. \tag{17}$$

The form of $\tilde{\mathbf{a}}_e$ in Eq. (17) is independent of the element length, thus $\partial \tilde{\mathbf{a}}_e/\partial \theta$ will be equal to zero for all parameters. To obtain the conditional derivative $\partial \mathbf{q}/\partial \theta|_{\mathbf{v}}$ according to the procedure established in the previous section, the element equilibrium and compatibility relationships are differentiated with respect to θ:

$$\frac{\partial \mathbf{q}}{\partial \theta} = \sum_{i=1}^{N_p} \tilde{\mathbf{a}}_e^T \frac{\partial \mathbf{s}}{\partial \theta} w_i, \tag{18a}$$

$$\frac{\partial \mathbf{e}}{\partial \theta} = \mathbf{a}_e \frac{\partial \mathbf{v}}{\partial \theta} + \frac{\partial \mathbf{a}_e}{\partial \theta} \mathbf{v}. \tag{18b}$$

The complete derivatives of the basic and section force vectors are

$$\frac{\partial \mathbf{q}}{\partial \theta} = \frac{\partial \mathbf{q}}{\partial \mathbf{v}} \frac{\partial \mathbf{v}}{\partial \theta} + \left.\frac{\partial \mathbf{q}}{\partial \theta}\right|_{\mathbf{v}}, \tag{18c}$$

$$\frac{\partial \mathbf{s}}{\partial \theta} = \frac{\partial \mathbf{s}}{\partial \mathbf{e}} \frac{\partial \mathbf{e}}{\partial \theta} + \left.\frac{\partial \mathbf{s}}{\partial \theta}\right|_{\mathbf{e}}. \tag{18d}$$

In Eq. (18a) use is made of the independence of $\tilde{\mathbf{a}}_e$ and w_i on θ. Analogous to the derivation for the conditional derivative of the element forces in the global system, the derivatives of the basic and section forces from Eqs. (18c) and (18d), respectively, are inserted in Eq. (18a). Then, Eq. (18b) is combined with the resulting expression and the definition of the element stiffness matrix in the basic system, $\mathbf{k}_b = \partial \mathbf{q}/\partial \mathbf{v}$, allows the cancellation of terms involving $\partial \mathbf{v}/\partial \theta$. This process results in the following equation for the conditional derivative in the displacement-based formulation:

$$\left.\frac{\partial \mathbf{q}}{\partial \theta}\right|_{\mathbf{v}} = \sum_{i=1}^{N_p} \left(\tilde{\mathbf{a}}_e^T \mathbf{k}_s \frac{\partial \mathbf{a}_e}{\partial \theta} \mathbf{v} + \tilde{\mathbf{a}}_e^T \left.\frac{\partial \mathbf{s}}{\partial \theta}\right|_{\mathbf{e}} \right) w_i, \tag{19}$$

where $\mathbf{k}_s = \partial \mathbf{s}/\partial \mathbf{e}$ is the section stiffness matrix. The vector, $\partial \mathbf{s}/\partial \theta|_{\mathbf{e}}$, is computed from the gradient of the section constitutive response, and it will be discussed later in this paper. The derivative, $\partial \mathbf{a}_e/\partial \theta$, is a straightforward scaling of the interpolation matrix in Eq. (14), where the only term that depends on θ is the common factor of $1/L$:

$$\frac{\partial \mathbf{a}_e}{\partial \theta} = -\frac{1}{L^2} \begin{bmatrix} 1 & 0 & 0 \\ 0 & 6x/L - 4 & 6x/L - 2 \end{bmatrix} \frac{\partial L}{\partial \theta} = -\mathbf{a}_e \frac{1}{L} \frac{\partial L}{\partial \theta}. \tag{20}$$

The derivative of the element length, $\partial L/\partial \theta$, is obtained by differentiating the direction cosines that describe the element orientation. This derivative is equal to zero when θ does not correspond to a coordinate of one of the element nodes. Further simplification of the conditional derivative of the basic forces is possible by inserting Eq. (20) into Eq. (19):

$$\left.\frac{\partial \mathbf{q}}{\partial \theta}\right|_{\mathbf{v}} = \sum_{i=1}^{N_\mathrm{P}} \tilde{\mathbf{a}}_\mathrm{e}^\mathrm{T} \left.\frac{\partial \mathbf{s}}{\partial \theta}\right|_\mathrm{e} w_i - \mathbf{k}_\mathrm{b}\mathbf{v}\frac{1}{L}\frac{\partial L}{\partial \theta}. \qquad (21)$$

The forms of Eqs. (20) and (21) are specific to the assumption of linear axial and cubic Hermitian transverse displacement fields, for which it is possible to normalize the interpolation matrix to $\tilde{\mathbf{a}}_\mathrm{e}$ in Eq. (17). This normalization makes for an efficient numerical implementation because it requires only one term in Eq. (21) to account for shape sensitivity in the basic system. Terms involving the derivative of $\mathbf{a}_\mathrm{e}$ will appear in the conditional derivative when displacement fields that are not normalized by the element length are assumed.

7. Gradient computations for force-based elements

In the force formulation [23], it is the compatibility relationship rather than equilibrium that is stated in integral form. The equilibrium and compatibility equations are $\mathbf{s} = \mathbf{b}\mathbf{q}$ and $\mathbf{v} = \int_0^L \mathbf{b}^\mathrm{T}\mathbf{e}\,\mathrm{d}x$, respectively, as indicated in Fig. 1. The matrix $\mathbf{b}$ interpolates section forces from the element end forces based on static equilibrium in the basic system:

$$\mathbf{b} = \begin{bmatrix} 1 & 0 & 0 \\ 0 & x/L - 1 & x/L \end{bmatrix}. \qquad (22)$$

Due to the normalization of the x-coordinate by the element length in Eq. (22), the force interpolation matrix does not depend on any parameter, therefore its derivative, $\partial \mathbf{b}/\partial \theta$, is equal to zero. The compatibility relationship is evaluated by numerical integration

$$\mathbf{v} = \sum_{i=1}^{N_\mathrm{P}} \mathbf{b}^\mathrm{T}(\xi_i)\mathbf{e}(\xi_i)\frac{L}{2}w_i. \qquad (23)$$

Neuenhofer and Filippou [18] developed a state determination procedure for force-based elements that bypasses the internal iterations required to satisfy the compatibility relationship in Eq. (23) while enforcing equilibrium at each section along the element. Gauss–Lobatto quadrature is standard for the implementation of force-based elements because it places integration points at the element ends where bending moments are known to be largest in the absence of element loads.

To establish the conditional derivative $\partial \mathbf{q}/\partial \theta|_{\mathbf{v}}$ in the force-based formulation, the equilibrium and compatibility relationships are differentiated with respect to θ:

$$\frac{\partial \mathbf{s}}{\partial \theta} = \mathbf{b}\frac{\partial \mathbf{q}}{\partial \theta}, \qquad (24a)$$

$$\frac{\partial \mathbf{v}}{\partial \theta} = \sum_{i=1}^{N_\mathrm{P}} \left(\mathbf{b}^\mathrm{T}\frac{\partial \mathbf{e}}{\partial \theta}\frac{L}{2} + \mathbf{b}^\mathrm{T}\mathbf{e}\frac{1}{2}\frac{\partial L}{\partial \theta} \right)w_i. \qquad (24b)$$

The complete derivatives of the basic and section force vectors are

$$\frac{\partial \mathbf{q}}{\partial \theta} = \frac{\partial \mathbf{q}}{\partial \mathbf{v}}\frac{\partial \mathbf{v}}{\partial \theta} + \left.\frac{\partial \mathbf{q}}{\partial \theta}\right|_{\mathbf{v}}, \qquad (24c)$$

$$\frac{\partial \mathbf{s}}{\partial \theta} = \frac{\partial \mathbf{s}}{\partial \mathbf{e}}\frac{\partial \mathbf{e}}{\partial \theta} + \left.\frac{\partial \mathbf{s}}{\partial \theta}\right|_\mathbf{e}. \qquad (24d)$$

The independence of $\mathbf{b}$ and w_i on θ is utilized in Eqs. (24a) and (24b). The process of combining equations to arrive at an expression for $\partial \mathbf{q}/\partial \theta|_{\mathbf{v}}$ is conceptually similar to that for the displacement-based formulation, but slightly more involved. First, the derivatives of the basic and section forces from Eqs. (24c) and (24d) are inserted in Eq. (24a). The resulting expression is rearranged to give an equation for $\partial \mathbf{e}/\partial \theta$:

$$\frac{\partial \mathbf{e}}{\partial \theta} = \mathbf{f}_\mathrm{s}\mathbf{b}\mathbf{k}_\mathrm{b}\frac{\partial \mathbf{v}}{\partial \theta} + \mathbf{f}_\mathrm{s}\mathbf{b}\left.\frac{\partial \mathbf{q}}{\partial \theta}\right|_{\mathbf{v}} - \mathbf{f}_\mathrm{s}\left.\frac{\partial \mathbf{s}}{\partial \theta}\right|_\mathbf{e}, \qquad (25)$$

where $\mathbf{f}_\mathrm{s} = \mathbf{k}_\mathrm{s}^{-1}$ is the section flexibility matrix. This expression is combined with Eq. (24b), then from the definition of the element flexibility matrix, $\mathbf{f}_\mathrm{b} = \int_0^L \mathbf{b}^\mathrm{T}\mathbf{f}_\mathrm{s}\mathbf{b}\,\mathrm{d}x$, and the identity $\mathbf{f}_\mathrm{b}\mathbf{k}_\mathrm{b} = \mathbf{I}$, the terms involving $\partial \mathbf{v}/\partial \theta$ cancel, and the final expression for the conditional derivative is

$$\left.\frac{\partial \mathbf{q}}{\partial \theta}\right|_{\mathbf{v}} = \mathbf{k}_\mathrm{b} \sum_{i=1}^{N_\mathrm{P}} \left(\mathbf{b}^\mathrm{T}\mathbf{f}_\mathrm{s}\left.\frac{\partial \mathbf{s}}{\partial \theta}\right|_\mathbf{e}\frac{L}{2} - \mathbf{b}^\mathrm{T}\mathbf{e}\frac{1}{2}\frac{\partial L}{\partial \theta} \right)w_i. \qquad (26)$$

From the element compatibility relationship of Eq. (23), further simplification of the conditional derivative is possible

$$\left.\frac{\partial \mathbf{q}}{\partial \theta}\right|_{\mathbf{v}} = \mathbf{k}_\mathrm{b} \sum_{i=1}^{N_\mathrm{P}} \mathbf{b}^\mathrm{T}\mathbf{f}_\mathrm{s}\left.\frac{\partial \mathbf{s}}{\partial \theta}\right|_\mathbf{e}\frac{L}{2}w_i - \mathbf{k}_\mathrm{b}\mathbf{v}\frac{1}{L}\frac{\partial L}{\partial \theta}. \qquad (27)$$

It is important to note the functional equivalence of Eqs. (21) and (27) for the displacement- and force-based formulations, respectively, where only one term is required to account for shape sensitivity of the element basic system.

Additional terms involving $\partial \mathbf{b}/\partial \theta$ appear in Eq. (27) when the interpolation of section shear forces is present; however, for the common case where shear effects are ignored, the form of Eq. (27) leads to an efficient numerical implementation because $\partial \mathbf{b}/\partial \theta$ is zero. The conditional derivative of the section forces, $\partial \mathbf{s}/\partial \theta|_\mathbf{e}$, depends on the constitutive model at each integration point along the element, as discussed in the following section.

8. Gradient computations at the section and material levels

The response at every cross-section along the element is defined in terms of the section deformations, $\mathbf{e}$, and the corresponding section forces, or stress resultants, $\mathbf{s}$, as indicated in Fig. 1. Regardless of the element formulation, the conditional derivative of the section forces, $\partial \mathbf{s}/\partial \theta|_\mathbf{e}$, is required to determine the element contribution to the gradient of the global resisting force vector, as seen in Eqs. (21) and (27). This derivative can be obtained by either direct differentiation of a closed-form stress-resultant plasticity relationship or by numerical integration of the material stress over the cross-section. In the former case, the

problem reduces to deriving analytic gradient equations for a section constitutive law; while in the latter case, the section compatibility and equilibrium equations, $\varepsilon = \mathbf{a}_s\mathbf{e}$ and $\mathbf{s} = \int_A \mathbf{a}_s^T \sigma \, dA$, respectively, must be differentiated. The cross-section integral is evaluated by numerical integration over a user-defined number of fibers, N_f:

$$\mathbf{s} = \sum_{i=1}^{N_f} \mathbf{a}_s^T \sigma_i A_i, \tag{28}$$

where the section compatibility matrix for the assumption of plane sections remain plane, $\mathbf{a}_s = [1 \; -y_i]$, contains the fiber locations, y_i. The material stress at the ith fiber location is σ_i, and A_i is the corresponding fiber area. Following the same procedure as in previous sections, the conditional derivative of the section forces is obtained by differentiating the section equilibrium and compatibility equations with respect to θ:

$$\frac{\partial \mathbf{s}}{\partial \theta} = \sum_{i=1}^{N_f} \left(\frac{\partial \mathbf{a}_s^T}{\partial \theta} \sigma_i A_i + \mathbf{a}_s^T \frac{\partial \sigma_i}{\partial \theta} A_i + \mathbf{a}_s^T \sigma_i \frac{\partial A_i}{\partial \theta} \right), \tag{29a}$$

$$\frac{\partial \varepsilon_i}{\partial \theta} = \mathbf{a}_s \frac{\partial \mathbf{e}}{\partial \theta} + \frac{\partial \mathbf{a}_s}{\partial \theta} \mathbf{e}. \tag{29b}$$

The complete derivatives of the section force vector and the material stress are

$$\frac{\partial \mathbf{s}}{\partial \theta} = \frac{\partial \mathbf{s}}{\partial \mathbf{e}} \frac{\partial \mathbf{e}}{\partial \theta} + \frac{\partial \mathbf{s}}{\partial \theta}\bigg|_{\mathbf{e}}, \tag{29c}$$

$$\frac{\partial \sigma_i}{\partial \theta} = \frac{\partial \sigma_i}{\partial \varepsilon_i} \frac{\partial \varepsilon_i}{\partial \theta} + \frac{\partial \sigma_i}{\partial \theta}\bigg|_{\varepsilon_i}, \tag{29d}$$

where ε_i is the strain at the ith fiber location. The substitution of the section force and material stress derivatives from Eqs. (29c) and (29d), respectively, into Eq. (29a) and subsequent combination of Eqs. (29a) and (29b) followed by cancellation of terms involving $\partial \mathbf{e}/\partial \theta$ via the section stiffness matrix, $\mathbf{k}_s$, gives the conditional derivative of the section forces

$$\frac{\partial \mathbf{s}}{\partial \theta}\bigg|_{\mathbf{e}} = \sum_{i=1}^{N_f} \left(\frac{\partial \mathbf{a}_s^T}{\partial \theta} \sigma_i A_i + \mathbf{a}_s^T k_m \frac{\partial \mathbf{a}_s}{\partial \theta} \mathbf{e} A_i + \mathbf{a}_s^T \frac{\partial \sigma_i}{\partial \theta}\bigg|_{\varepsilon_i} A_i + \mathbf{a}_s^T \sigma_i \frac{\partial A_i}{\partial \theta} \right), \tag{30}$$

where $k_m = \partial \sigma / \partial \varepsilon$ is the material stiffness. The derivatives $\partial \mathbf{a}_s / \partial \theta$ and $\partial A_i / \partial \theta$ correspond to variations in the location and size, respectively, of the ith fiber in the cross-section. These terms are important in computing the structural response sensitivity to the dimensions and details of member cross-sections. The computations of $\partial \mathbf{a}_s / \partial \theta$ and $\partial A_i / \partial \theta$ are demonstrated in Appendix I for a fiber-discretized wide flange section. A similar approach is performed for reinforced concrete sections in which it is particularly important to determine the response sensitivity to the amount and placement of steel reinforcement, as demonstrated in the numerical examples at the end of this paper.

The remaining task in computing the structural response sensitivity is to obtain $\partial \sigma_i / \partial \theta|_{\varepsilon_i}$ for the material response at each fiber location. A number of references provide detailed derivations of the response sensitivity for particular constitutive laws, including Zhang and Der Kiureghian [25], Kleiber et al. [13], Roth and Grigoriu [20], and Haukaas and Der Kiureghian [8]. Implementations in OpenSees include the J_2 plasticity model and a number of uniaxial material models for inelastic behavior of steel and concrete.

9. Response gradients with respect to global shape parameters

The derivations in the previous sections include element response sensitivities with respect to nodal coordinates. However, it is frequently of interest to obtain sensitivities with respect to global shape parameters, which include the end coordinates of frame members that are discretized into several finite elements, as well as parameters that describe the global geometrical imperfection of a structure. Thus, the perturbation of a global shape parameter will perturb several nodal coordinates.

To obtain response sensitivities with respect to a global shape parameter, an explicit relationship between the dependent nodal coordinates, $\widetilde{\boldsymbol{\Theta}}$, and the shape parameters is required. For the case of one shape parameter, denoted $\tilde{\theta}$, which may coincide with a nodal coordinate of a member, this relationship is the expressed as

$$\widetilde{\boldsymbol{\Theta}} = f(\tilde{\theta}), \tag{31}$$

where $\widetilde{\boldsymbol{\Theta}}$ is the set of nodal coordinates that depend on the global shape parameter $\tilde{\theta}$.

As an example, consider a straight multi-element member with n nodes in 2-D space. The coordinates of the member ends are denoted (x_1, y_1) and (x_n, y_n). Any of these four parameters can be the parameter $\tilde{\theta}$ for which the response sensitivity is sought. To establish the explicit form of Eq. (31), the other nodal coordinates of the member are expressed in terms of the end coordinates:

$$x_i = x_1 + (x_n - x_1)\frac{i-1}{n-1}, \quad i = 1, 2, \ldots, n, \tag{32a}$$

$$y_i = y_1 + (y_n - y_1)\frac{i-1}{n-1}, \quad i = 1, 2, \ldots, n, \tag{32b}$$

where $n-1$ is the number of elements into which the member is discretized.

To obtain response sensitivities with respect to the global shape parameter, the chain rule of differentiation is applied to the nodal response sensitivity:

$$\frac{\partial \mathbf{U}}{\partial \tilde{\theta}} = \frac{\partial \mathbf{U}}{\partial \widetilde{\boldsymbol{\Theta}}} \frac{\partial \widetilde{\boldsymbol{\Theta}}}{\partial \tilde{\theta}}. \tag{33}$$

The matrix $\partial \mathbf{U}/\partial \widetilde{\boldsymbol{\Theta}}$ is available from the derivations in previous sections, while the vector $\partial \widetilde{\boldsymbol{\Theta}}/\partial \tilde{\theta}$ is obtained by differentiation of Eq. (31). For the example in Eq. (32), when the sensitivity of a response quantity u is sought with respect to the x-coordinate of node 1 of the member, Eq. (33) becomes

$$\frac{\partial u}{\partial x_1} = \sum_{i=1}^{n} \frac{\partial u}{\partial x_i} \left(1 - \frac{i-1}{n-1} \right). \tag{34}$$

When $\tilde{\theta}$ represents a global structural shape imperfection, the vector $\partial \widetilde{\Theta} / \partial \tilde{\theta}$ is established by computing the imperfection at each node due to a unit global imperfection. Thus, the vector $\partial \widetilde{\Theta} / \partial \tilde{\theta}$ is interpreted as a vector of influence coefficients.

Global structural shape imperfections, as well as the end coordinates of multi-element members are uncertain quantities. Thus, they should be considered as random variables in a structural reliability analysis, as demonstrated in the following numerical examples of a steel and a reinforced concrete frame.

10. Numerical examples

The response sensitivity equations derived in this paper have been implemented in OpenSees and verified by finite difference calculations. To investigate the importance of uncertain geometrical imperfections relative to other uncertain structural parameters, static pushover reliability analyses are performed for two types of structures: a steel frame and a reinforced concrete frame. Static pushover analysis is the prevalent analysis approach for capacity assessment in earthquake engineering since it assesses the ability of the structure to reach a target displacement demand. Hence, the analyses in this paper are intended to address probabilistic assessments of structural capacity.

10.1. Finite element reliability analysis of steel structure

The first structure considered is the three-bay, three-story steel frame in Fig. 2. Each member is discretized into four displacement-based elements to represent the nonlinear distribution of curvature along the member length. A fiber-discretization represents the response of the wide-flange steel cross-sections of the frame members, as shown

in Fig. 2. There are two fibers in each flange and ten fibers in the web. The stress–strain behavior of each steel fiber is represented by the uniaxial material model shown in Fig. 5a, for which there are three material parameters: (1) elastic modulus, E; (2) yield strength, f_y; and (3) second-slope stiffness ratio, α.

All material and geometric parameters of the structural model are considered uncertain. The dimensions d, t_w, b_f, and t_f of the cross-section of each member are modeled as uncorrelated normal random variables with means 250, 20, 250, and 20 mm, respectively, and 2% coefficient of variation (cov). The elastic modulus, E, of each member is a lognormal random variable with mean 200,000 MPa, 5% cov, and correlation coefficient 0.6 with the elastic modulus of the other members. The steel yield strength, f_y, of each member is a lognormal random variable with mean 300 MPa, 10% cov, and correlation coefficient 0.6 with f_y of the other members. The stiffness ratio, α, of each member is a lognormal random variable with mean 0.02, 10% cov, and correlation coefficient 0.6 with α of the other members. In total, 21 members × 7 parameters = 147 random variables represent the material and cross-section geometry parameters. Additionally, the two coordinates of each of the 16 connection nodes are considered to be uncorrelated normal random variables, giving a grand total of 179 random variables. The standard deviation of the vertical coordinates is 10 mm, while the standard deviation of the horizontal coordinates varies from 10 mm at the base to 25 mm at the roof. The variation of the standard deviation with the height is due to the potential for a global sway of the building due to geometrical imperfection. It is noted that each member is assumed to remain straight, that is, the location of the internal member nodes is described by Eq. (32).

To investigate the importance of geometrical imperfections relative to other structural parameters deterministic loads are applied to the structure. The gravity loads are 50 kN at the external connections and 100 kN at internal
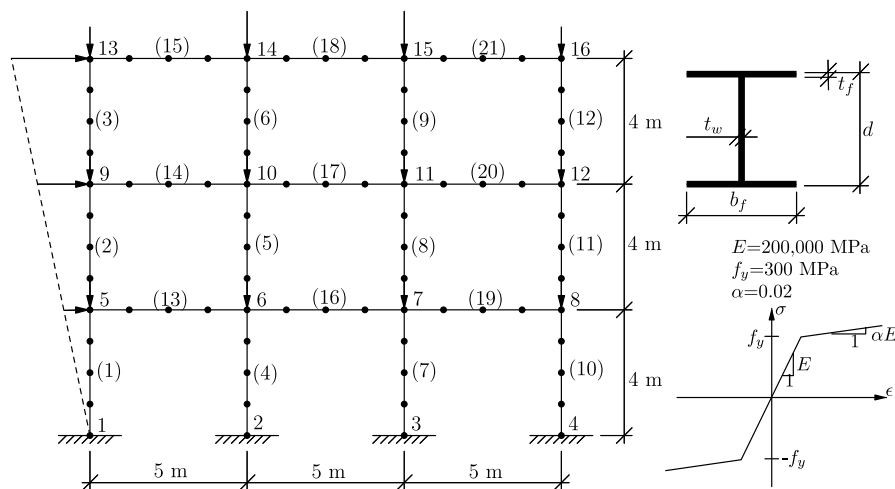

Fig. 2. Steel frame structure. Node numbers and element numbers (in parentheses) are shown.

connections. The lateral loads vary with the height as shown in Fig. 2, with maximum value 400 kN at the roof level.

To assess the lateral displacement demand on the structure, a finite element reliability analysis is undertaken in order to obtain the probability that the total drift of the roof exceeds 3%. The performance function for this response event is

$$g = 3\% \times 12\,\mathrm{m} - u_{13}, \tag{35}$$

where u_{13} is the horizontal displacement at node 13. The MPP in the FORM analysis is obtained after five evaluations of the performance function and its gradient. That is, five runs of the finite element analysis with different realizations of the random variables are required. The resulting reliability index, β, is 2.01, which implies a 0.022 probability of exceeding the 3% target drift. Fig. 3 shows the displacement response at node 13 versus the load factor at the mean realization and the MPP realization of the random variables. As expected, moderate nonlinearity is observed at the mean, while significant yielding occurs at the failure displacement.

Of particular interest in this paper is the ranking of the random variables according to the importance measure in Eq. (5). The 25 most important variables as the 179 random variables are shown in Table 1. The yield strengths of the column members, except that of member 12, which ranks 34th, rank among the most important parameters. This emphasizes the fact that yielding takes place in the columns in this example. The web depth, d, and flange width, b_f, of several column members rank 12 through 25 in Table

Table 1
Ranking of the 25 most important parameters in the steel frame example

Object	Parameter	γ-Value
Member 5	f_y	−0.38034
Member 7	f_y	−0.37828
Member 3	f_y	−0.32439
Member 2	f_y	−0.32253
Member 10	f_y	−0.27291
Member 6	f_y	−0.27279
Member 9	f_y	−0.26853
Member 4	f_y	−0.22111
Member 1	f_y	−0.2168
Member 8	f_y	−0.13287
Member 11	f_y	−0.13264
Member 5	d	−0.11495
Member 7	d	−0.11403
Member 3	d	−0.10055
Member 2	d	−0.09987
Member 10	d	−0.08305
Member 9	d	−0.08215
Member 6	d	−0.08194
Member 5	b_f	−0.07104
Member 7	b_f	−0.07054
Member 1	d	−0.07005
Member 4	d	−0.06978
Member 3	b_f	−0.0614
Member 2	b_f	−0.061
Member 5	t_f	−0.05928

1, indicating the importance of imperfections in the cross-section geometry, even with the low cov of 2%. The horizontal coordinates of nodes 4, 8, and 12 in the right column line rank among the 50 most important random variables,
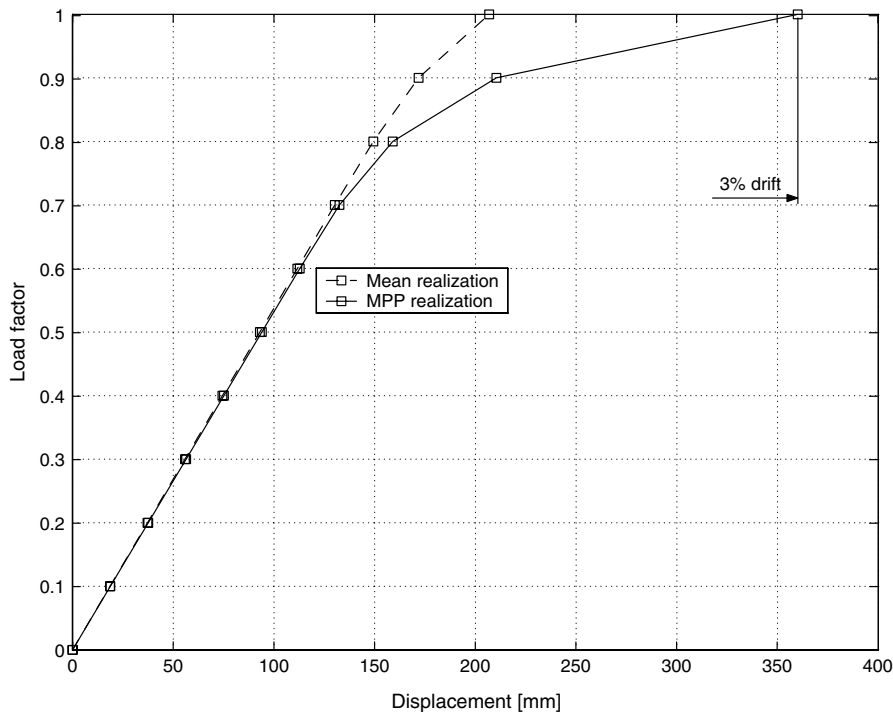

Fig. 3. Load–displacement response at the mean and MPP realizations of the random variables for the steel structure.

thus indicating a relatively high importance of imperfection in the global geometry of the structure.

10.2. Finite element reliability analysis of reinforced concrete structure

It is of interest to investigate whether the observations made for the steel frame are also valid for a reinforced concrete frame. For this purpose, a reliability analysis of the two-bay, two-story structure in Fig. 4 is performed. Each frame member is represented by a single force-based element to capture the variation in curvature that results from the interaction of axial and moment forces. Each fiber in the cross-sections shown in Fig. 4 is modeled by a uniaxial material model. The core and cover concrete material fibers are described by a uniaxial model with a modified Kent–Park backbone curve [21] with zero stress in tension and linear unloading/reloading, as shown in Fig. 5b and c, respectively. The bilinear model used in the previous example represents the stress–strain response of the reinforcing steel.

All material and geometry parameters are considered uncertain. The cross-sectional dimensions b and h of the members are uncorrelated normal random variables with the mean values given in Fig. 4 and 5% cov. The area of each reinforcing bar is a normal random variable with
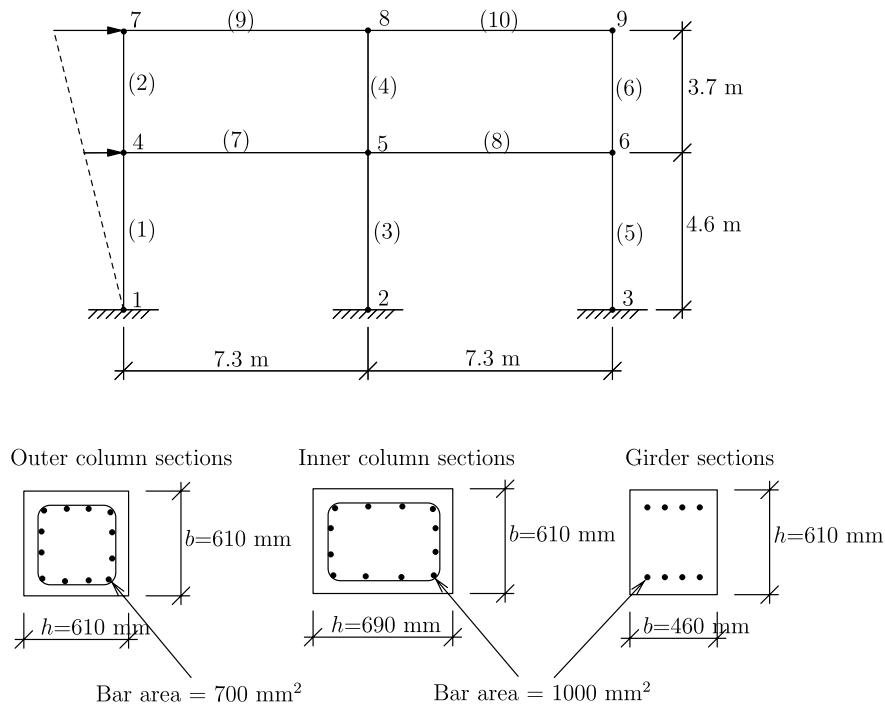

Fig. 4. Reinforced concrete frame structure. Node numbers and element numbers (in parentheses) are shown.
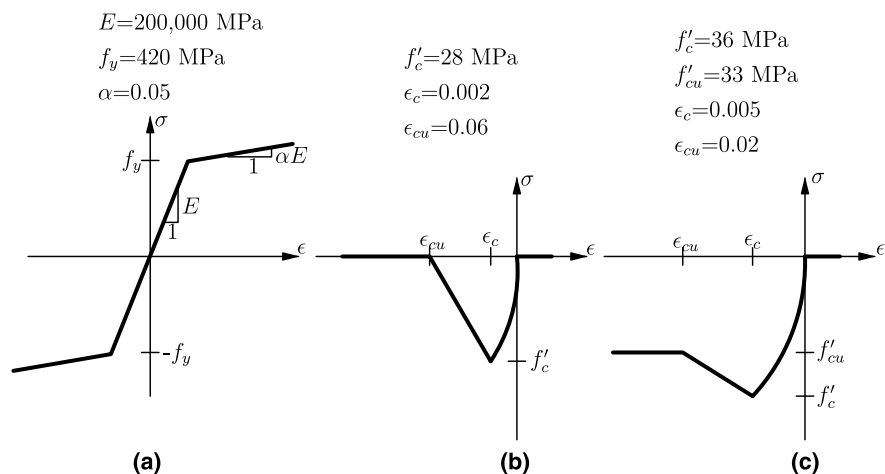

Fig. 5. Material models for (a) steel, (b) unconfined concrete in girders and column cover regions, and (c) confined concrete in column core regions.
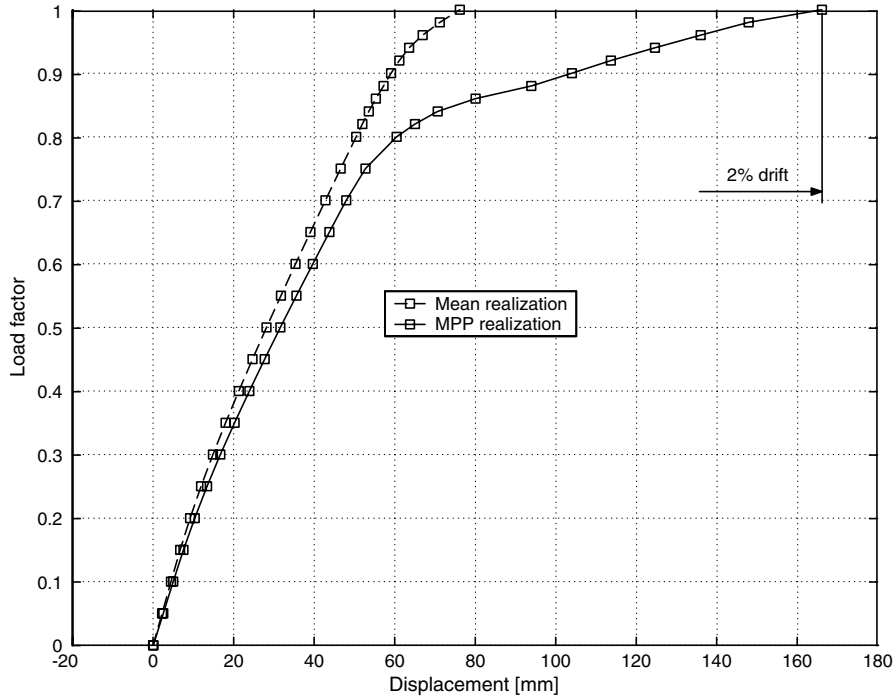
Fig. 6. Load–displacement response at the mean and MPP realizations of the random variables for the reinforced concrete structure.

the mean value shown in Fig. 4 and 2% cov. The thickness of the cover concrete in each member is a normal random variable with mean 75 mm and 10% cov.

The elastic modulus, E, of the reinforcing steel of each member is a lognormal random variable with mean 200,000 MPa, 5% cov, and correlation coefficient 0.6 with E of the other members. The reinforcing steel yield strength, f_y, for each member is a lognormal random variable with mean 420 MPa, 10% cov, and correlation coefficient 0.6 with f_y of the other members. The stiffness ratio, α, of the reinforcing steel of each member is a lognormal random variable with mean 0.05, 10% cov, and correlation coefficient 0.6 with α of the other members. All concrete material parameters in Fig. 5b and c are lognormal random variables with the mean values shown in the figures and 10% cov. The concrete strength parameters, f_c' and f_{cu}', are inter-correlated by 0.6, as are the corresponding strains, ε_c and ε_{cu}. The two coordinates of each node are considered to be uncorrelated normal random variables. The vertical coordinates are assigned a standard deviation of 10 mm, while the horizontal coordinates are assigned standard deviations that vary from 10 mm at the base to 20 mm at the roof. There are a total of 142 random variables for this reliability analysis. The gravity loads are $G_4 = G_6 = G_8 = 850$ kN, $G_5 = 1700$ kN, and $G_7 = G_9 = 430$ kN, while the lateral loads are $P_4 = 450$ kN and $P_7 = 900$ kN. All of the applied loads are deterministic.

The performance function for this example is defined to determine the probability the roof displacement will exceed 2% drift:

$$g = 2\% \times 8.3 \text{ m} - u_7, \tag{36}$$

where u_7 is the lateral displacement of node 7. A FORM finite element reliability analysis converges in nine iterations to the reliability index 2.76 with corresponding probability 0.0029. Significant nonlinearity occurs at the most likely failure realization of the random variables, as shown

Table 2
Ranking of the 25 most important parameters in the reinforced concrete frame example

Object	Parameter	γ-Value
Member 3	h	−0.34697
Member 7	h	−0.34339
Member 4	h	−0.32343
Member 8	h	−0.31364
Member 4	f_y	−0.2853
Member 5	h	−0.24275
Member 8	f_y	−0.23581
Member 7	f_y	−0.23421
Member 3	f_y	−0.17896
Member 3	Cover depth	0.15903
Member 1	h	−0.15483
Member 4	Cover depth	0.14254
Member 7	Cover depth	0.1311
Member 5	Cover depth	0.12401
Member 4	ε_{cu}^{cover}	0.12336
Member 8	Cover depth	0.12045
Member 5	f_y	−0.12021
Member 1	f_y	−0.09227
Node 2	x-coordinate	−0.0902
Member 1	Cover depth	0.07958
Node 5	x-coordinate	0.07674
Member 10	f_y	−0.07497
Member 4	$f_c'^{core}$	0.07103
Member 9	f_y	−0.06721
Node 3	x-coordinate	−0.06562

in Fig. 6. The 25 most important random variables are listed in Table 2. Remarkably, it is found that the cross-section height h of the members adjacent to the inner connection are the most important parameters, followed by the yield strength of the reinforcing steel of the same members. These results indicate a high influence of geometrical imperfections on the reliability of the reinforced concrete structure. It is also noted that the depth of the cover concrete ranks high in importance. This finding may justify further investigation of the dispersion in the amount of cover in reinforced concrete structures. As in the previous example, the global structural shape imperfection represented by the horizontal nodal coordinates also ranks high in importance with nodes 2, 3, and 5 listed among the 25 most important random variables.

11. Conclusions

A comprehensive and unified treatment of response sensitivity equations by the direct differentiation method was developed. Geometric, material, and load parameters are included in both the force-based and the displacement-based formulations of inelastic beam-column response. Sensitivity equations for global shape parameters account for geometric imperfections of structural members discretized into multiple finite elements. The analytical equations have been implemented and verified in the OpenSees software. The finite element reliability analysis of a three-bay, three-story steel frame demonstrated the member cross-sectional dimensions, particularly the section depth and the flange width, rank high in importance. For the two-bay, two-story reinforced concrete structure, the cross-section depth, as well as the thickness of the cover concrete, are important parameters relative to the material parameters. In each example, the importance ranking of geometrical imperfections relative to other structural parameters indicates a significant influence of uncertain geometrical parameters on reliability assessments, even when the dispersion in the probability distribution is small.

Appendix I. Wide flange section shape sensitivity equations

As indicated in Eq. (30), it is necessary to compute the derivatives $\partial \mathbf{a}_s/\partial\theta$ and $\partial A_i/\partial\theta$ at each fiber location in order to account for variations in the geometric parameters that define a fiber-discretized cross-section. The derivative of
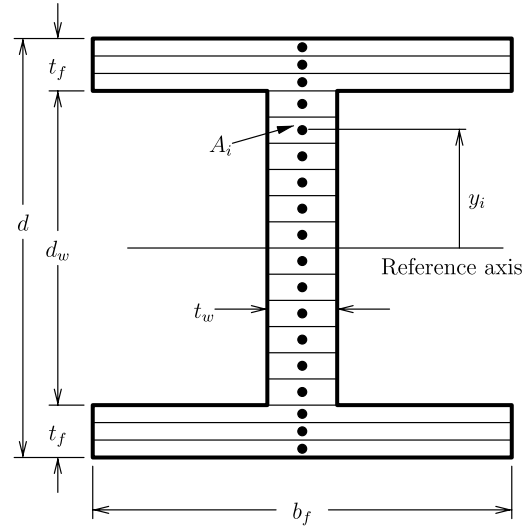

Fig. 7. Wide flange section dimensions and fiber discretization.

the section compatibility matrix at the ith fiber location is $\partial \mathbf{a}_s/\partial\theta = [0 \quad -\partial y_i/\partial\theta]$.

The section is defined by the following geometric parameters, as shown in Fig. 7 the overall section depth, d; the web thickness, t_w; the flange width, b_f; and the flange thickness, t_f. The number of fibers through the depth of the web is N_{fw}, and N_{ff} is the number of fibers through the thickness of each flange. Each of the derivatives, $\partial d/\partial\theta$, $\partial t_w/\partial\theta$, $\partial b_f/\partial\theta$, and $\partial t_f/\partial\theta$ is equal to either one or zero depending on the property θ represents in the structural model. Both N_{fw} and N_{ff} are deterministic parameters.

I.1. Web fibers

From the section dimensions and the number of fibers, the area of each fiber in the web is the web area divided by the number of web fibers:

$$A_w = \frac{d_w t_w}{N_{fw}}, \tag{37}$$

where the depth of the web, d_w is

$$d_w = d - 2t_f. \tag{38}$$

The distance from the reference axis to the centroid of the ith web fiber is

$$y_i = \left(\frac{d}{2} - t_f\right) - \left(i - \frac{1}{2}\right)\frac{d_w}{N_{fw}}, \quad i = 1,\ldots,N_{fw}. \tag{39}$$

The differentiation of Eq. (37) with respect to θ gives the sensitivity of the size of the web fibers to the parameter

$$\frac{\partial A_w}{\partial\theta} = \frac{1}{N_{fw}}\left(d_w\frac{\partial t_w}{\partial\theta} + \frac{\partial d_w}{\partial\theta}t_w\right), \tag{40}$$

where the sensitivity of the web depth is

$$\frac{\partial d_w}{\partial\theta} = \frac{\partial d}{\partial\theta} - 2\frac{\partial t_f}{\partial\theta}. \tag{41}$$

Similarly, the differentiation of Eq. (39) gives the sensitivity of the web fiber centroid locations

$$\frac{\partial y_i}{\partial \theta} = \left(\frac{1}{2} \frac{\partial d}{\partial \theta} - \frac{\partial t_{\mathrm{f}}}{\partial \theta} \right) - \left(i - \frac{1}{2} \right) \frac{1}{N_{\mathrm{fw}}} \frac{\partial d_{\mathrm{w}}}{\partial \theta}, \quad i = 1, \ldots, N_{\mathrm{fw}}. \tag{42}$$

I.2. Flange fibers

For the fibers in the flange regions, the size of each fiber is

$$A_{\mathrm{f}} = \frac{b_{\mathrm{f}} t_{\mathrm{f}}}{N_{\mathrm{ff}}}, \tag{43}$$

and the centroid location of the ith fiber is

$$y_i = \frac{d}{2} - \left(i - \frac{1}{2} \right) \frac{t_{\mathrm{f}}}{N_{\mathrm{ff}}}, \quad i = 1, \ldots, N_{\mathrm{ff}}. \tag{44}$$

The sensitivity of the size of each flange fiber to θ is

$$\frac{\partial A_{\mathrm{f}}}{\partial \theta} = \frac{1}{N_{\mathrm{ff}}} \left(b_{\mathrm{f}} \frac{\partial t_{\mathrm{f}}}{\partial \theta} + \frac{\partial b_{\mathrm{f}}}{\partial \theta} t_{\mathrm{f}} \right), \tag{45}$$

while the sensitivity of the ith flange fiber centroid location is

$$\frac{\partial y_i}{\partial \theta} = \frac{1}{2} \frac{\partial d}{\partial \theta} - \left(i - \frac{1}{2} \right) \frac{1}{N_{\mathrm{ff}}} \frac{\partial t_{\mathrm{f}}}{\partial \theta}, \quad i = 1, \ldots, N_{\mathrm{ff}}. \tag{46}$$

References

[1] Bjerager P, Krenk S. Parameter sensitivity in first order reliability theory. J Eng Mech 1989;115(7):1577–82.

[2] Choi KK, Santos JLT. Design sensitivity analysis of non-linear structural systems, Part I: Theory. Int J Numer Meth Eng 1987;24: 2039–55.

[3] Conte JP, Vijalapura PK, Meghella M. Consistent finite element sensitivity in seismic reliability analysis. In: Proceedings of 13th ASCE engineering mechanics division conference, Baltimore, MD. The Johns Hopkins University; 1999.

[4] Filippou FC, Fenves GL. Methods of analysis for earthquake-resistant structures. In: Bozorgnia Y, Bertero VV, editors. Earthquake engineering: from engineering seismology to performance-based engineering. Boca Raton, FL: CRC Press; 2004 [chapter 6].

[5] Franchin P. Reliability of uncertain inelastic structures under earthquake excitation. J Eng Mech 2004;130(2):180–91.

[6] Hamburger R, Rojahn C, Moehle J, Bachman R, Comartin C, Whittaker A. The atc-58 project: development of next-generation performance-based earthquake engineering decision criteria for buildings. In: Proceedings of the 13th world conference on earthquake engineering (13th WCEE), Vancouver, Canada; 2004.

[7] Haukaas T, Der Kiureghian A. Developments in finite element reliability and sensitivity analysis of nonlinear structures. In: Der Kiureghian A, Madanat S, Pestana J, editors. Proceedings of the ninth international conference on applications of statistics and probability in civil engineering, ICASP9, San Francisco, California; 2003.

[8] Haukaas T, Der Kiureghian A. Finite element reliability and sensitivity methods for performance-based engineering. Report No. PEER 2003/14, Pacific Earthquake Engineering Research Center, University of California, Berkeley, CA; 2004.

[9] Haukaas T, Der Kiureghian A. Parameter sensitivity and importance measures in nonlinear finite element reliability analysis. J Eng Mech 2005;131(10):102.

[10] Hohenbichler M, Rackwitz R. Non-normal dependent vectors in structural safety. J Eng Mech 1981;107(6):1227–38.

[11] Hohenbichler M, Rackwitz R. Sensitivity and importance measures in structural reliability. Civil Eng Syst 1986;3:203–9.

[12] Hughes TJR. The finite element method: linear static and dynamic finite element analysis. Englewood Cliffs, NJ: Prentice Hall; 1987.

[13] Kleiber M, Antunez H, Hien T, Kowalczyk P. Parameter sensitivity in nonlinear mechanics. West Sussex, UK: John Wiley and Sons Ltd.; 1997.

[14] Liu P-L, Der Kiureghian A. Multivariate distribution models with prescribed marginals and covariances. Probabilist Eng Mech 1986;1(2):105–12.

[15] Liu P-L, Der Kiureghian A. Finite element reliability of geometrically nonlinear uncertain structures. J Eng Mech 1991;17(8):1806–25.

[16] McKenna F, Fenves GL, Scott MH. Open system for earthquake engineering simulation. Pacific Earthquake Engineering Research Center, University of California, Berkeley, CA; 2003. Available from http://opensees.berkeley.edu/.

[17] Moehle J, Deierlein GG. A framework methodology for performance-based earthquake engineering. In: Proceedings of the 13th world conference on earthquake engineering (13th WCEE), Vancouver, Canada; 2004.

[18] Neuenhofer A, Filippou FC. Evaluation of nonlinear frame finite-element models. J Struct Eng 1997;123(7):958–66.

[19] Rosenblatt M. Remarks on a multivariate transformation. Ann Math Stat 1952;23:470–2.

[20] Roth C, Grigoriu M. Sensitivity analysis of dynamic systems subjected to seismic loads. Report No. MCEER-01-0003, Multidisciplinary Center for Earthquake Engineering Research, State University of New York, Buffalo, NY; 2001.

[21] Scott BD, Park R, Priestley MJN. Stress–strain behavior of concrete confined by overlapping hoops at low and high strain rates. ACI J. 1982;79(1).

[22] Scott MH, Franchin P, Fenves GL, Filippou FC. Response sensitivity for nonlinear beam-column elements. ASCE J Struct Eng 2004; 130(9):1281–8.

[23] Spacone E, Ciampi V, Filippou FC. Mixed formulation of nonlinear beam finite element. Comput Struct 1996;58:7183.

[24] Tsay JJ, Arora JS. Nonlinear structural design sensitivity analysis for path dependent problems. Part 1: General theory. Comput Meth Appl Mech Eng 1990;81:183–208.

[25] Zhang Y, Der Kiureghian A. Dynamic response sensitivity of inelastic structures. Comput Meth Appl Mech Eng 1993;108:23–36.

[26] Zienkiewicz O, Taylor R. The finite element method. 5th ed. Oxford, Boston: Butterworth-Heinemann; 2000.